

## Fragmentation of $^{14,15}\text{N}_2$ by electron impact investigated using a time-delayed spectroscopic technique

Natalia Ferreira,<sup>1</sup> L. Sigaud,<sup>1</sup> V. L. B. de Jesus,<sup>2</sup> A. B. Rocha,<sup>3</sup> L. H. Coutinho,<sup>1</sup> and E. C. Montenegro<sup>1</sup>

<sup>1</sup>*Instituto de Física, Universidade Federal do Rio de Janeiro, Caixa Postal 68528 Rio de Janeiro, BR-21945-970, RJ, Brazil*

<sup>2</sup>*Instituto Federal de Educação, Ciência e Tecnologia do Rio de Janeiro (IFRJ), Campus Nilópolis, R. Lucio Tavares 1045, BR-26530-060 Nilópolis, RJ, Brazil*

<sup>3</sup>*Instituto de Química, Universidade Federal do Rio de Janeiro Cidade Universitária–Ilha do Fundão, BR-21941-909, RJ, Brazil*

(Received 15 March 2012; published 5 July 2012)

A general method to measure the energy distribution function of molecular fragments using a pulsed electron beam with time-delayed extraction coupled to a time-of-flight spectrometer is presented. The energy distributions of the homoisotopic species  $^{14,15}\text{N}^+$  and  $^{14,15}\text{N}_2^{2+}$ , with the same mass-to-charge ratio, produced by 35–400 eV electron impact ionization of  $\text{N}_2$ , are disentangled, showing two independent fragmentation routes for  $\text{N}^+$  ions with kinetic energies smaller than 1.0 eV. No measurable isotopic effect was found, indicating that predissociation does not play a role in this region of impact energies.

DOI: [10.1103/PhysRevA.86.012702](https://doi.org/10.1103/PhysRevA.86.012702)

PACS number(s): 34.80.Gs, 34.70.+e

### I. INTRODUCTION

Molecular dissociation is a common phenomenon which produces atoms and ions that are orders of magnitude more reactive than the original molecule. The plethora of new chemical species produced in planetary atmospheres [1–3] or of biological species which are destroyed due to the strong reactivity of the hydroxyl radicals produced by ionizing radiation [4–7] are consequences of the creation of highly reactive species from the fragmentation of common molecules such as hydrogen, nitrogen, oxygen or water, among others. Nitrogen is especially important since it is the largest constituent of our atmosphere. The atmosphere of Titan, which is considered to resemble Earth's in primordial times, also has  $\text{N}_2$  as its major constituent [8–11]. Dissociation of  $\text{N}_2$  by electron impact plays an underlying role for the chemical inventory of the upper atmosphere of Titan [2], as this moon remains for a large part of its trajectory immersed in the magnetosphere of Saturn [10,11].

Ions are often produced in molecular fragmentation if one of its inner valence electrons is removed. The rearrangement of the remaining electrons gives rise to bound or repulsive potentials, whose asymptotic values and its details in the Franck-Condon region will determine the final kinetic energy of the released ion. The resulting kinetic energy distribution (KED) extends from zero up to several tens of eV, if the molecule is multiply ionized. In the case of  $\text{N}_2$ , the part of the KED corresponding to the most energetic ions has been measured by several authors using electrons and heavy ions as impinging particles, with fairly conclusive results of the main groups that make up the distribution [10–15]. For low-energy released ions ( $E \leq 1.0$  eV), the scenario is much poorer as the need to combine accurate detection efficiency, good energy resolution, and separation of ions with the same mass-to-charge ratio is not easily achieved using techniques associated with mass spectrometry [14,16].  $\text{N}_2^{2+}$  falls in this case because it is a stable ion with the same mass-to-charge ratio as  $\text{N}^+$  and is produced at thermal energies. This lack of information prevents progress on some of the topics mentioned above. Indeed, as the escape energy of the N atom from Titan is  $\sim 0.3$  eV [10,11], quantitative knowledge of the low-energy part of the KED is needed to determine the escape flow and to

identify some possible isotopic contributions to this flux. The ratio  $^{15}\text{N}/^{14}\text{N}$  in Titan's atmosphere presents anomalies that are not yet fully understood [17–19].

Molecular fragmentation gives rise to low-energy ions through mechanisms like excitation to the vibrational continuum or pre-dissociation. In the case of  $\text{N}_2$ , predissociation is believed to involve the coupling of the vibrational levels of the  $C^2\Sigma_u^+$  state with the vibrational continuum of the  $B^2\Sigma_u^+$  state [20]. This has been investigated through charge transfer collisions, radiative decay, and photoionization and has been considered as the main dissociation mechanism near the threshold by several authors [20–23]. However, the role of predissociation in fragment ion production by electron or heavy-particle impact is still unclear.

Emission of low-energy N ions by electron impact becomes dominant as the impact energy decreases and approaches the fragmentation threshold [12]. If predissociation is the most important mechanism in the fragmentation of  $\text{N}_2$  induced by low-energy electrons, a large isotopic dependence for the released ions might be expected. Indeed, measurements performed by Govers *et al.* [22] with 90-eV electrons indicate that the predissociation efficiency for  $^{14}\text{N}$  may be about 10 times higher than for the  $^{15}\text{N}$ . These measurements recorded UV radiation from the  $C^2\Sigma_u^+$  to the  $X^2\Sigma_g$  states of the  $\text{N}_2^+$ . Determination of possible isotope effect through a direct measurement of the released N ions would have a strong influence on other areas of knowledge, as mentioned.

On the other hand, fragmentation due to excitation to vibrational continuum should present almost no isotopic effect. The measurement of the low-energy part of the KED for dissociation of  $^{14}\text{N}_2$  and  $^{15}\text{N}_2$  by electron impact can determine the route of dissociation of the molecule as well as if there is any isotopic selectivity for the ion production rate. To this end, a methodology capable to discriminate groups of low-energy ions of different species with the same mass ( $m$ ) to charge ( $q$ ) ratio and good efficiency of detection was developed.

### II. EXPERIMENT

The experimental technique is based on a time-of-flight (TOF) mass spectrometer, coupled to an electron gun, where

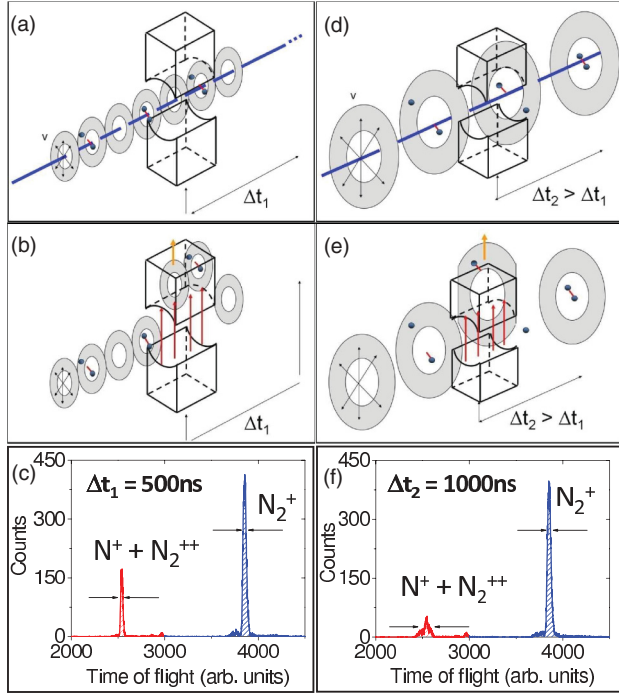


FIG. 1. (Color online) Diagrammatic representation and examples of the resulting spectra of the free-flight evolution of the ions. After a short delay time  $\Delta t_1$  (a) most of the ions produced in the interaction region are detected when the extraction pulse is turned on [(b) and (c)]. For a longer delay time  $\Delta t_2$  (d), the most energetic ions have left the interaction region when the extraction pulse is turned on (e) and are not detected (f). Ions with  $v \simeq D/(2\Delta t_2)$  are partially detected. The  $N^+ + N_2^{2+}$  peak ( $m/q = 14,15$ ) is significantly decreased with respect to the  $N_2^+$  ( $m/q = 28,30$ ) in (f) as compared to (c).

the interaction occurs within a cell where the gas of interest is kept in thermal equilibrium with the environment. The electron beam pulse is interspersed with the extraction pulse, which can be activated after the passage of the electron beam pulse with a

controlled time delay, acting as a velocity selector. A standard coincidence electronics operated with start pulses supplied from the extraction pulser and stop pulses from the recoil ion multichannel plate detector provided the TOF spectra. The velocity distribution function of the ions is obtained by the detection of the number of ions as a function of the delay time, in conjunction with a modeling of the free flight of the ions from the interaction zone until the moment when the extraction pulse is turned on (see Fig. 1).

The experimental arrangement used in the present work has been described previously [24] and it is shown diagrammatically in Fig. 2. In the present measurements we used 50-ns electron beam pulses with a frequency of 20 kHz. The extraction pulse has 700-V amplitude and 10- $\mu$ s width. The geometry of the extraction region inside the gas cell gives a capacitive load to the extraction pulse electronics resulting in an intrinsic minimum delay of 500 ns due to the pulse rise time. This is the main factor for the decrease of the transmission efficiency for  $N^+$  ions with kinetic energy above 3.0 eV. The measurements scanned delays from that minimum up to 10  $\mu$ s. The electron beam diameter is  $d = 0.8$  mm and the conical aperture connecting the gas cell with the TOF tube has  $D = 6.0$ -mm diameter. The work pressure inside the cell was  $\sim 1 \times 10^{-4}$  Torr. The best performance of the spectrometer occurs for low velocity ions, when the transmission efficiency is essentially independent of their kinematic details.

Assuming cylindrical symmetry with respect to the beam axis, the number of recorded ions,  $n_{\text{Rec}}(\Delta t)$ , as a function of the delay time  $\Delta t$  can be expressed in terms of a transmission efficiency  $n_T(v_{\perp}, \Delta t)$ , which is a function of the delay time and of the transverse velocity of the ion  $v_{\perp}$ , and of the velocity distribution function  $f(v_{\perp})$  as

$$n_{\text{Rec}}(\Delta t) = \int_0^{\infty} n_T(v_{\perp}, \Delta t) f(v_{\perp}) dv_{\perp}. \quad (1)$$

The transmission efficiency  $n_T(v_{\perp}, \Delta t)$  can be analytically obtained from the geometry of the extraction region and the kinematics of the free-flying ion. It is given by

$$n_T(v_{\perp}, \Delta t) = 2D^2 \left\{ \frac{D}{2} \left[ \frac{\arcsin(u_{\min})}{2u_{\min}^2} - \frac{\arcsin(u_{\max})}{2u_{\max}^2} \right] + \frac{\sqrt{1-u_{\min}^2}}{2u_{\min}} - \frac{\sqrt{1-u_{\max}^2}}{2u_{\max}} \right\} + v_{\perp} \Delta t \left[ \frac{\arcsin(u_{\min})}{u_{\min}} - \frac{\arcsin(u_{\max})}{u_{\max}} \right] - v_{\perp} \Delta t \left[ \ln \left| \frac{1 + \sqrt{1-u_{\min}}}{u_{\min}} \right| - \ln \left| \frac{1 + \sqrt{1-u_{\max}}}{u_{\max}} \right| \right], \quad (2)$$

where  $u_{\min} = D/(2v_{\perp}\Delta t + d)$ ,  $u_{\max} = D/(2v_{\perp}\Delta t)$ , and its accuracy was checked through the SIMION package [25]. Due to the high extraction voltage used, it can be approximated as a step function  $n_T(v_{\perp}, \Delta t) = 1$  if  $v_{\perp}\Delta t \leq D/2$  and zero otherwise. This approximation is useful to understand the main features of the measured  $n_{\text{Rec}}(\Delta t)$ .

Equation (1) is a Fredholm-type integral equation where  $n_{\text{Rec}}(\Delta t)$  and  $n_T(v_{\perp}, \Delta t)$  are known and  $f(v_{\perp})$  is generally unknown, as in the case of the  $m/q = 14,15$  groups of ions. We handle that by assuming as trial functions three Gaussians, and one exponential and one Maxwell-Boltzmann

(MB) distribution to compose  $f(v_{\perp})$  and minimize the  $R^2$  difference with respect to the measured  $n_{\text{Rec}}(\Delta t)$  by the appropriate choice of the distribution parameters. The three Gaussians centered at 0.8, 3.0–4.0, and 8.0 eV account for the main groups of  $N^+$  ions reported by some authors for electron and heavy-ion impact [10–15]; the exponential distribution was used by Ben-Itzhak *et al.* [26] to describe the dissociation of  $H_2^+$  via vibrational continuum and accounts for  $N^+$  ions released with kinetic energies near zero, and the MB distribution accounts for the  $N_2^{2+}$  ions. Figure 3 illustrates the physical origin of these groups.

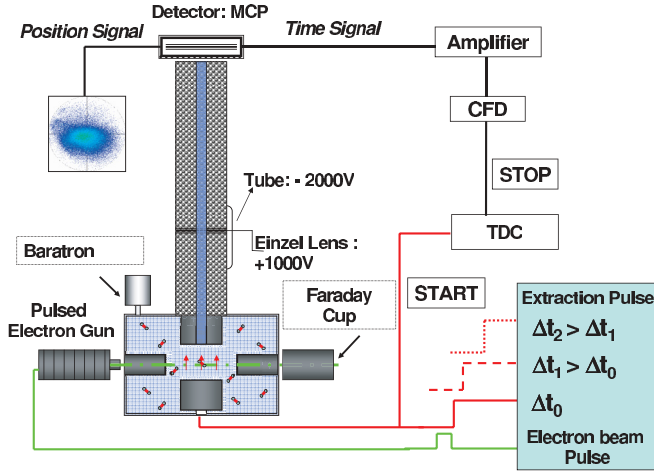


FIG. 2. (Color online) Diagrammatic representation of the experimental arrangement. The extraction pulse, which is delayed with respect to the electron beam pulse by an adjustable amount, gives the TOF start signal. In Ref. [24] a constant delay,  $\Delta t_0$ , synchronized to turn on the extraction pulse just after the passage of the electron beam pulse, was used.

In the case of the Maxwell-Boltzmann distribution,  $f(E) = (2\sqrt{E}/\sqrt{\pi})\alpha^{3/2}e^{-\alpha E}$ ,  $\alpha = 1/kT$ , and

$$f(v_{\perp})dv_{\perp} = 2\gamma^2 e^{-\gamma^2 v_{\perp}^2} v_{\perp} dv_{\perp}, \quad (3)$$

with  $\gamma^2 = \alpha m/2$  and  $m$  being the ion mass.

For the Gaussian ( $f(E) = Ae^{-\alpha^2(E-E_0)^2}$ ) and exponential (Expo) ( $Ae^{-\alpha E}$ ) energy distribution functions, numerical integration over the velocity component parallel to the beam axis  $v_{\parallel}$  is needed to express the trial functions in terms of  $v_{\perp}$ ,

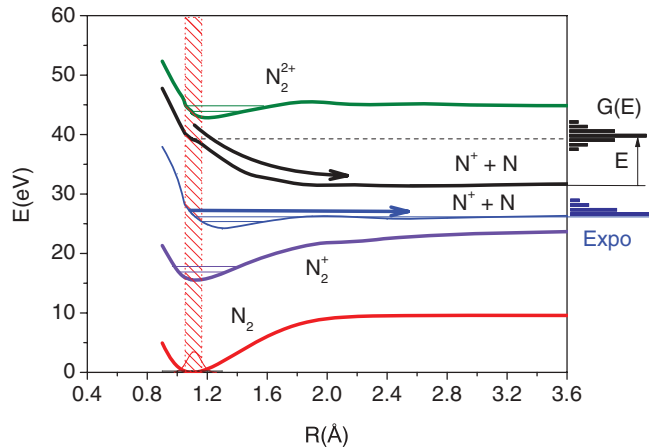


FIG. 3. (Color online) Illustration of molecular orbitals of  $\text{N}_2$  and of some dissociative mechanisms. The hatched rectangle corresponds to the Franck-Condon region. Ionization from the ground state of  $\text{N}_2$  can result in stable molecular ions, such as  $\text{N}_2^+$  or  $\text{N}_2^{2+}$ , or in dissociation, either through a repulsive potential, or through the vibrational continuum. The stable molecular ions,  $\text{N}_2^+$  or  $\text{N}_2^{2+}$ , have a Maxwell-Boltzmann distribution. The repulsive case results in a Gaussian distribution while, in the continuum vibrational case, the  $\text{N}^+$  ions can be described by an exponential distribution.

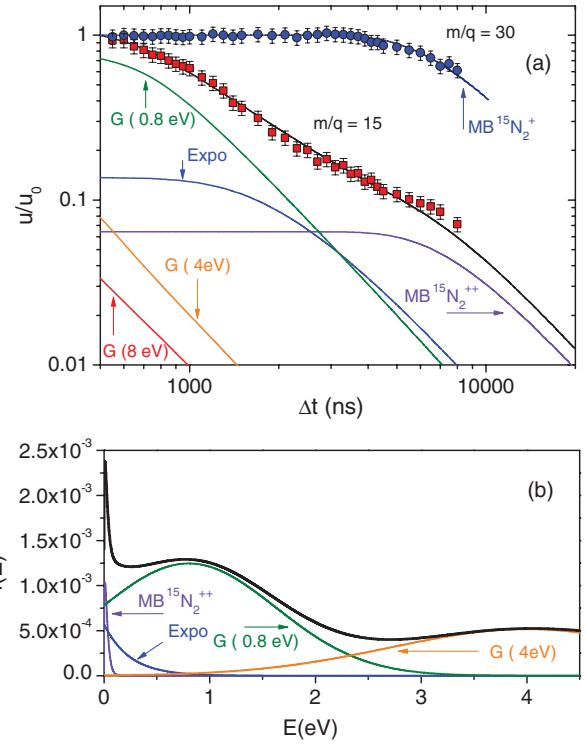


FIG. 4. (Color online) (a) Measured  $u/u_0$  for 100-eV electrons on  $^{15}\text{N}_2$  as a function of the delay  $\Delta t$  for both  $m/q = 30$  and  $m/q = 15$ . For  $m/q = 30$  a single Maxwell-Boltzmann (MB) distribution describes the data, while for  $m/q = 15$  the measurements are fitted by the five distributions shown. (b) The energy distribution functions used in (a) for the  $m/q = 15$  case are displayed as a function of the translational kinetic energy of the ion. Expo denotes the exponential distribution and  $G(E)$  denotes Gaussians centered at energy  $E$ .

and can be written, respectively, as

$$f(v_{\perp})dv_{\perp} = (Am/2)v_{\perp}dv_{\perp} \times \int_{-\infty}^{\infty} e^{-\gamma^4(v_{\perp}^2 + v_{\parallel}^2 - v_0^2)^2} (v_{\parallel}^2 + v_{\perp}^2)^{-1/2} dv_{\parallel}, \quad (4)$$

with  $v_0 = \sqrt{2E_0/m}$ , and

$$f(v_{\perp})dv_{\perp} = (Am/2)v_{\perp}dv_{\perp} \times \int_{-\infty}^{\infty} e^{-\gamma^2(v_{\perp}^2 + v_{\parallel}^2)} (v_{\parallel}^2 + v_{\perp}^2)^{-1/2} dv_{\parallel}. \quad (5)$$

In these last two cases  $A$  and  $\alpha$  are free parameters.

It should be noted that, for electron impact ionization, a large number of molecular orbitals with different symmetries (due to the role played by the ejected electron) can be populated in the final state, and alignment effects of the fragments with respect to the electron beam direction are not expected to be important.

### III. RESULTS AND DISCUSSION

The ratios  $u/u_0 = n_{\text{Rec}}(\Delta t)/n_{\text{Rec}}(500 \text{ ns})$  for 100 eV electrons on  $^{15}\text{N}_2$  as a function of the delay  $\Delta t$  are shown in Fig. 4(a), for both the  $^{15}\text{N}_2^+$  ( $m/q = 30$ ) and  $^{15}\text{N}^+ + ^{15}\text{N}_2^{2+}$  ( $m/q = 15$ ) groups of ions. For the  $^{15}\text{N}_2^+$ , a unique MB distribution at room temperature is enough to describe the

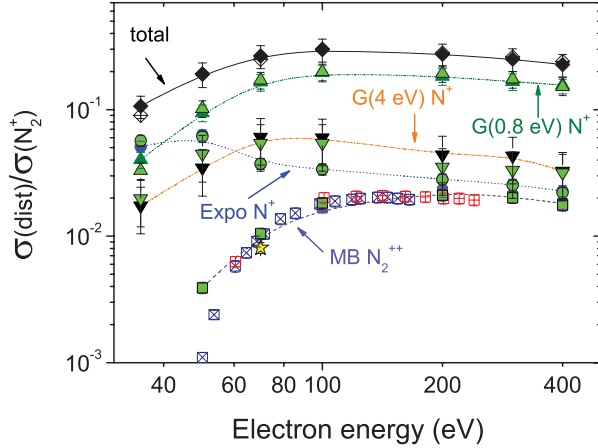


FIG. 5. (Color online) Cross-section ratios of the distributions composing the  $m/q = 14$  (black solid symbols) and  $15$  (green solid symbols) groups, and  $^{14,15}\text{N}_2^+$ . Data from Refs. [27] ( $^{14}\text{N}^{15}\text{N}$ ), [28] ( $^{14}\text{N}^{15}\text{N}$ ), and [16] ( $^{14}\text{N}_2$ ) for  $\text{N}_2^{2+}$  are shown by cross-filled squares, x-filled squares, and a star, respectively. The sum of all ratios (total) for  $^{14}\text{N}_2$  are compared with the single-coincidence measurements of Ref. [29] (cross-filled lozenges). Lines are drawn to guide the eye.

measured data very well. The main points to be emphasized for the  $m/q = 15$  group are as follows: (i) The high-energy Gaussians (at 4 and 8 eV) have small influence on the measured ratio due to the loss of a substantial part of these ions in our apparatus; (ii) the three low-energy distributions have different shapes which are all necessary to reproduce the measured  $u/u_0$  along the whole range of  $\Delta t$  scanned; (iii) basically, the MB determines the shape of  $u/u_0$  for large  $\Delta t$ , the Gaussian at 0.8 eV for small  $\Delta t$ , and the exponential controls the amount of the concavity change around  $\Delta t \sim 2\text{--}3 \mu\text{s}$ ; (iv) there is little freedom for the energy regions where these three groups of ions should appear to properly reproduce  $u/u_0$ ; (v) these are essentially the minimum number of distributions able to describe the measurements and the inclusion of a larger number of distributions does not change the overall picture; (vi) the same scenario occurs for the 50, 200, 300, and 400 eV impinging electron energies. For 35-eV electrons, which are below the double ionization threshold ( $\sim 43$  eV), a slight change of  $G(4.0$  eV) to  $G(3.0$  eV) is needed to give the same quality of fitting. The decrease of the mean energy of this Gaussian occurs because the higher lying molecular orbitals are not effectively populated as the electron energy decreases. The weighted energy distributions thus obtained for  $m/q = 15$  as a function of the translational kinetic energy of the ions is shown in Fig. 4(b). The total distribution has a similar shape of those presented by other authors [10–15,21]. The values of  $1/\alpha$  for the distributions  $G(4.0$  eV),  $G(0.8$  eV), and exponential are 1.82, 1.20, and 0.24 eV, respectively, for both isotopes. The average kinetic energy of the low-energy, exponential group, is thus 0.24 eV.

Thus,  $\text{N}_2^{2+}$  and  $\text{N}^+$  ions, which have the same mass-to-charge ratio, can be fully separated in a TOF-based measurement. The low-energy  $\text{N}^+$  ions belong to two different groups with different spectroscopic signatures in respect to the translational kinetic energy distributions.

TABLE I. Ratios between the cross section associated with each of the energy distributions and the cross section of the parent molecule,  $10^2\sigma(\text{distrib.})/\sigma(^{14}\text{N}_2^+)$ , for ions with  $m/q = 14$ , at the measured electron energies. For 35 eV the  $G(3.0$  eV) was used instead of  $G(4.0$  eV) (see text).

$E$ (eV)	$\text{N}_2^{2+}$ (MB)	Exponential	$G(0.8$ eV)	$G(4.0$ eV)
35		$5.11 \pm 0.51$	$4.0 \pm 0.6$	$1.7 \pm 0.7$
50	$0.39 \pm 0.04$	$6.29 \pm 0.63$	$9.4 \pm 1.4$	$3.5 \pm 1.4$
70	$1.05 \pm 0.11$	$3.73 \pm 0.37$	$16.5 \pm 2.5$	$6.1 \pm 2.4$
100	$1.69 \pm 0.17$	$3.38 \pm 0.34$	$19.5 \pm 2.9$	$6.0 \pm 2.4$
200	$2.25 \pm 0.22$	$2.82 \pm 0.28$	$18.3 \pm 2.7$	$4.4 \pm 1.8$
300	$2.04 \pm 0.20$	$2.56 \pm 0.26$	$16.6 \pm 2.5$	$4.3 \pm 1.7$
400	$1.81 \pm 0.18$	$2.28 \pm 0.23$	$15.6 \pm 2.4$	$3.3 \pm 1.3$

These findings are stressed in Fig. 5, where the contribution from each distribution to the  $m/q = 14$  or  $15$  products, relative to  $^{14,15}\text{N}_2^+$ , are shown as a function of the electron energy. The measured ratios between the cross section associated with each of the energy distributions and the cross section of the parent molecule for ions with  $m/q = 14$  and  $m/q = 15$  are given in Tables I and II, respectively. Our  $^{14,15}\text{N}_2^{2+}/^{14,15}\text{N}_2^+$  homoisotopic ratios are compared with measurements using heteroisotopic  $^{14}\text{N}^{15}\text{N}$  molecules [27,28] and with the homoisotopic  $^{14}\text{N}_2$  measurement of Shiki *et al.* [16] at 70 eV, with very good general agreement. To the authors' knowledge, besides Ref. [16], which uses a cryogenic detection system, there are no other previous measurements reporting the  $\text{N}_2^{2+}/\text{N}_2^+$  ratio for homoisotopic species. For a consistency verification, the sum of all ratios (total) for  $^{14}\text{N}_2$  is compared to the single-coincidence measurements of Tian and Vidal [29], also showing very good agreement.

The fragmentation dynamics leading to  $\text{N}^+$  ions with near-zero kinetic energy (exponential) is very different from  $G(0.8$  eV) (Fig. 5). Although the KED cannot be measured in great detail, the present method is able to quantify the cross sections associated with the two main groups of  $\text{N}^+$  ions with kinetic energies  $\leq 1.0$  eV and identify significant differences in their dependence with the electron energy.

The energy dependencies of the  $G(0.8$  eV) and exponential distributions with the impact energy suggest that the former is composed by contributions from repulsive potentials with small energy differences between their values at the Franck-

TABLE II. Ratios between the cross section associated with each of the energy distributions and the cross section of the parent molecule,  $10^2\sigma(\text{distrib.})/\sigma(^{15}\text{N}_2^+)$ , for ions with  $m/q = 15$ , at the measured electron energies. For 35 eV the  $G(3.0$  eV) was used instead of  $G(4.0$  eV) (see text).

$E$ (eV)	$\text{N}_2^{2+}$ (MB)	Exponential	$G(0.8$ eV)	$G(4.0$ eV)
35		$5.71 \pm 0.57$	$3.3 \pm 0.4$	$2.0 \pm 0.8$
50	$0.39 \pm 0.04$	$6.11 \pm 0.61$	$10.2 \pm 1.5$	$4.5 \pm 1.8$
70	$1.05 \pm 0.11$	$3.73 \pm 0.37$	$17.1 \pm 2.6$	$5.4 \pm 2.2$
100	$1.83 \pm 0.17$	$3.38 \pm 0.34$	$19.9 \pm 3.0$	$5.4 \pm 2.2$
200	$2.11 \pm 0.22$	$2.81 \pm 0.28$	$19.3 \pm 2.9$	$3.5 \pm 1.4$
300	$2.01 \pm 0.20$	$2.53 \pm 0.25$	$17.4 \pm 2.6$	$3.3 \pm 1.3$
400	$1.76 \pm 0.18$	$2.21 \pm 0.21$	$15.2 \pm 2.3$	$3.2 \pm 1.3$

Condon region and the asymptotic limit, while the latter, which has a maximum at a lower impact energy than the  $\text{N}_2^+$ , is originated from direct [21] or autoionizing [30] transitions ending up in some of the lower  $\Pi_g$  states whose vibrational continuum is accessible within the Franck-Condon region [30] (see Fig. 3). It should be recalled that, in the case of impact of low-energy electrons, molecular orbitals of any symmetry can be populated because essentially no selection rule is applicable [31,32]. In the measured range of impact energies, the preponderance of these mechanisms precludes the observation of the predissociation channel and, within the present uncertainties, of any isotopic effect associated with it.

#### IV. CONCLUSIONS

To conclude, the quantitative disentanglement of the  $m/q = 14,15$  groups of ions here obtained imposes new constraints for a still lacking theoretical approach to the long-lasting question concerning electron impact fragmentation of  $\text{N}_2$  delivering low-energy ions. Fragmentation of homoisotopic  $^{14}\text{N}_2^+$  or  $^{15}\text{N}_2^+$  shows two groups of low-energy ions with different dynamical signatures emerging. No measurable isotopic effect was found, indicating that predissociation does not play a role in this region of impact energies. This is a relevant issue, not only to uncover the electron-impact fragmentation dynamics of  $\text{N}_2$ , but also due to its influence on the isotopic fractionation

and on the escape flux of N in Titan. The only previous measurement—to our knowledge—able to separate the  $\text{N}^+$  and  $\text{N}_2^{2+}$  ions (same mass-to-charge ratio in homoisotopic molecules), and to provide a quantitative value for the  $\text{N}_2^{2+}$  cross section (Ref. [16]), used a complex cryogenic detector, which restricts its use at large. Absolute cross sections for the various distributions can be readily obtained from the parent ion production. Furthermore, the methodology here introduced opens new perspectives for mass spectrometry based on the well-established TOF technique. Other doubly charged ions such as  $\text{C}_2\text{H}_2^{2+}$ , which has the same  $m/q$  ratio of  $\text{CH}^+$ , and which could not be separated with standard TOF setups, can have their stability investigated. The separation of ionic products  $\text{N}_2^+$  and  $\text{CO}^+$ —with the same  $m/q$ —from mixtures of gases like  $\text{N}_2$  and  $\text{CO}_2$  can be also accomplished in situations where the standard TOF limitations cannot be circumvented by the artificial use of isotopes, like in space probes, for example.

#### ACKNOWLEDGMENTS

Support from Brazilian Agencies Conselho Nacional de Desenvolvimento Científico e Tecnológico (CNPq), Coordenação de Aperfeiçoamento de Pessoal de Nível Superior (CAPES) and Fundação de Amparo à Pesquisa do Rio de Janeiro (FAPERJ). The authors gratefully acknowledge the valuable help by W. Wolff.

- 
- [1] W. Klemperer, *Annu. Rev. Phys. Chem.* **62**, 173 (2011).
  - [2] P. Lavvas *et al.*, *Icarus* **213**, 233 (2011).
  - [3] H. Imanaka and M. A. Smith, *Proc. Natl. Acad. Sci. USA* **107**, 28 (2010).
  - [4] B. Halliwell, *Lancet* **344**, 721 (1994).
  - [5] K. R. Hogstrom and P. R. Almond, *Phys. Med. Biol.* **51**, R455 (2006).
  - [6] H. Luna and E. C. Montenegro, *Phys. Rev. Lett.* **94**, 043201 (2005).
  - [7] E. C. Montenegro, M. B. Shah, H. Luna, S. W. J. Scully, A. L. F. Barros, J. A. Wyer, and J. Lecointre, *Phys. Rev. Lett.* **99**, 213201 (2007).
  - [8] H. B. Niemann *et al.*, *Nature (London)* **438**, 779 (2005).
  - [9] J. H. Waite Jr. *et al.*, *Science* **316**, 870 (2007).
  - [10] H. Luna *et al.*, *J. Geophys. Res.* **108**, 5033 (2003).
  - [11] M. B. Shah *et al.*, *Astrophys. J.*, **703**, 1947 (2009).
  - [12] L. J. Kieffer and R. J. Van Brunt, *The J. Chem. Phys.* **46**, 2728 (1967).
  - [13] R. Loch, J. Schopman, H. Wankenne, and J. Momigny, *Chem. Phys.* **7**, 393 (1975).
  - [14] R. J. Van Brunt and L. J. Kieffer, *J. Chem. Phys.* **63**, 3216 (1975).
  - [15] A. K. Edwards, R. M. Wood, and M. F. Steuer, *Phys. Rev. A* **15**, 48 (1977).
  - [16] S. Shiki *et al.*, *J. Mass Spectrom.* **43**, 1686 (2008).
  - [17] H. Lammer, W. Stumtner, G. J. Molina-Cuberos, S. J. Bauer, and T. Owene, *Planet. Space Sci.* **48**, 529 (2000).
  - [18] M.-C. Liang, A. N. Heays, B. R. Lewis, S. T. Gibson, and Y. L. Yung, *Astrophys. J.* **664**, L115 (2007).
  - [19] B. Bezard, *Philos. Trans. R. Soc. London A* **367**, 683 (2009).
  - [20] C. Nicolas, C. Alcaraz, R. Thissen, M. Vervloet, and O. Dutuit, *J. Phys. B: At. Mol. Opt. Phys.* **36**, 2239 (2003).
  - [21] P. Fournier *et al.*, *Chem. Phys. Lett.* **9**, 426 (1971).
  - [22] T. R. Govers, C. A. van de Runstraat, and F. J. de Heer, *J. Phys. B: Atom. Molec. Phys.* **6**, L73 (1973).
  - [23] P. Erman, *Phys. Scr.* **14**, 5 (1976).
  - [24] L. Sigaud *et al.*, *J. Phys. B: At. Mol. Opt. Phys.* **43**, 105203 (2010).
  - [25] [<http://www.simion.com>].
  - [26] I. Ben-Itzhak *et al.*, *J. Phys. B: At. Mol. Opt. Phys.* **29**, L21 (1996).
  - [27] N. R. Daly and R. E. Powell, *Proc. Phys. Soc.* **89**, 273 (1966).
  - [28] T. D. Mark, *J. Chem. Phys.* **63**, 3731 (1975).
  - [29] C. Tian and C. R. Vidal, *J. Phys. B: At. Mol. Opt. Phys.* **31**, 5369 (1998).
  - [30] T. Aoto *et al.*, *J. Chem. Phys.* **124**, 234306 (2006).
  - [31] G. H. Dunn, *Phys. Rev. Lett.* **8**, 62 (1962).
  - [32] W. A. Goddard, D. L. Huestis, D. C. Cartwright, and S. Trajmar, *Chem. Phys. Lett.* **11**, 329 (1971).